ELSEVIER

Journal of Contaminant Hydrology 18 (1995) 239–255

JOURNAL OF
Contaminant
Hydrology

# Moisture content effect on radon emanation in porous media

Hongbing Sun *, David J. Furbish

*Department of Geology, Geophysical Fluid Dynamics Institute, The Florida State University, Tallahassee, FL 32306, USA*

Received 1 March 1994; accepted after revision 9 January 1995

**Abstract**

It is impractical to establish the detailed recoil range distribution and to measure the rough recoil surface of the porous media experimentally. Thus a computer based modelling approach is followed. The ion collision theory of nuclear physics provides the basics for calculating the recoil range distributions for radon within solid, water and air. The collision history is established by the modified Monte Carlo TRIM program. The recoil emanation power can also be calculated from the recoil range distributions. The recoil surface areas of the porous media are calculated through the fractal quantification of the synthetic porous media. The embedding effects are numerically calculated for solid, water and air, the three coexisting phases. The moisture distribution in the porous media is discussed based on the capillary theory. The simulation results indicate that the radon emanation rate is positively correlated with the moisture saturation in the porous media. The greater the moisture saturation is, the greater the possible radon emanation rate is. With moisture contents from 10% up to 30%, the recoil emanation rates quickly reach the emanation rate of the saturated condition. As the moisture reaches 30%, a universal thin film on the pore surface is formed. This thin film is sufficient to stop the recoil radon from embedding into another part of the pore wall. The existing experimental data support this result.

## 1. Introduction

The goal of this study is to learn more about the relationship between radon emanation in porous media and the moisture content. This knowledge is particularly important in relation to radon as a health problem, and the use of radon in process investigation. Variation in moisture saturation in soils has been recognized as a cause for fluctuating radon concentration in indoor air (Brookins, 1990). Fluctuation radon

* Corresponding author.


*SSDI* 0169-7722(95)00002-X

concentrations might be partly responsible for the false indications of earthquakes in the monitoring systems. Radon release from the porous media has been used by some researchers as a tracer for tracing groundwater seepage into the ocean because generally radon concentrations are higher in groundwater than marine water (Drever, 1988). All of this considerations point to the importance of the radon–water–air studies (Tanner, 1980; Bossus, 1984; Semkow, 1990,1991; Paulsen, 1991).

Radon is an $\alpha$-decay product. There are two major radon isotopes measured in nature, $^{222}$Rn and $^{220}$Rn. $^{222}$Rn is the $\alpha$-decay product of $^{226}$Ra in the $^{238}$U series decay chain; $^{220}$Rn is the $\alpha$-decay product of $^{226}$Ra in the $^{232}$Th series decay chain. Both the $^{238}$U and $^{232}$Th occur naturally in minor concentrations in porous media. The basic mechanism of radon escape from the solid material has been summarized by Tanner (1980) as $\alpha$-recoil, where the radon atoms are mobilized from the solid material due to the recoil energy of $\alpha$-decay.

The study of recoil release of the radon from the solid material first involves studying the emanating power of the radon from the host material. The emanating power is the chance of a radon ion recoiling out from the solid surface. A second area of interest is in studying the recoil surface area which involves the fractal quantification of the surface area of a porous medium. After the radon recoil out, because of the left-over recoil energies, it interacts with the water film and the air in the pore. A third area of concern therefore, is to consider the buffering effect of water and air for trapping the emanated radon particles.

There have been intensive experimental studies on the occurrence of the radon in indoor air and groundwater, and the relationship between moisture variation and radon fluctuation (Thamer et al., 1982). However, no studies have systematically examined how moisture variations result in radon concentration fluctuation. Theoretical interpretations are difficult because it is impractical to track down the individual recoil ion and to calculate the recoil range distribution experimentally. It is also an intimidating task to measure the rough surface of the porous media. Therefore, a simulation based approach is more practical and productive. First, this paper presents the model determination of the recoil ion paths within the solid material, and calculating of the emanating power. Next, it examines the emanating surface area, and the net effect of water and air in trapping the recoil radon in pores. These theoretical calculations provide the basis for establishing the relation of moisture saturation change and radon radioactive change. In a final section of the paper, the predicted radioactive ratio will be compared with a group of known experimental data.

## 2. Monte Carlo simulation of recoil range distribution and emanating power of radon

$^{222}$Rn is the $\alpha$-decay product of $^{226}$Ra, and $^{220}$Rn is the $\alpha$-decay product of $^{224}$Ra. Upon decay, the mass differences between the parent and daughter elements are converted into decay energies. The decay and recoil energies can be calculated according to the mass differences of the parents, daughters and $\alpha$-particles before and after decay. The decay energy of radon is $\sim 4$ MeV. Most of the decay energies goes to the

$\alpha$-particles and only a small portion goes to the recoil daughters. For $^{222}$Rn, the recoil energy is 86.24 keV and for $^{220}$Rn, the recoil energy is 102.96 keV.

The process of energized daughter recoil in porous media is similar to the process of ion implantation into successive layers of material. The differences are that the recoiling daughter receives its energy from decay, and a possible layer of the target material might be air or water as opposed to another layer of solid material. This feature makes it possible for a recoil process to be simulated with the modification of a Monte Carlo ion implantation program TRIM (Ziegler et al., 1985). The TRIM refers to "Transport of Ion in Matter", and was developed for determining the ion range and damage distributions as well as angular and energy distributions of backscattered and transmitted ions. The method involves following a large number of individual ion collision "histories" in a target. Each history begins with a given energy, position and direction. The ion energy is reduced as a result of nuclear and electronic (inelastic) losses; a collision history is terminated either when the energy drops below a pre-specified value or when the ion is out of the target. The nuclear and electronic energy losses or stopping powers are assumed to be independent. Thus, particles lose energy in discrete amounts in nuclear collisions and lose energy continuously from electronic interactions. Input parameters include: atomic number and weight, recoil energy (in keV), number of ions to be recoiled, recoil angle (incident angle), displacement energy; for the target material, these include target material thickness and density; and atomic number and weight, and relative amounts of target elements. The output from the modified TRIM program includes recoil range distributions projected in $x$-, $y$- and $z$-directions, and the distance $R$ from the initial position along with means and standard deviations. The recoil range distribution data for a single ion from modified TRIM program are necessary for calculating the recoil probability (Fig. 1).

The modified TRIM output gives the recoil range distribution from a fixed initial position. For the radon recoil, the recoil initial positions and directions are random in the solid. These initial random positions and random recoil directions need to be considered for calculating the emanating power. Therefore an additional Monte Carlo simulation is required. The algorithm first generates the recoil range according to the recoil range frequency distribution (Fig. 1) calculated from modified TRIM. After the recoil range $R$ is generated, a random recoil angle (three-dimensional, 3-D) is selected to compute the component of the recoil range normal to the solid–fluid surface. This component value is compared with the initial distance of the recoil ion to the solid–fluid surface. If the former is greater, then we consider the ion to have recoiled out. The total number of ions recoiled out from the solid surface divided by the total number of recoils occurring within the solid is the probability that a single ion will recoil out of the solid. This probability is the emanating power. This emanating power (Table 1; Fig. 2) will be used to calculate the emanation rate in Section 4.

## 3. Fractal recoil surface area of synthetic porous media

After the recoil range distributions and emanating powers are calculated, the recoil surface area needs to be calculated. This surface area can be studied over the synthetic porous media.

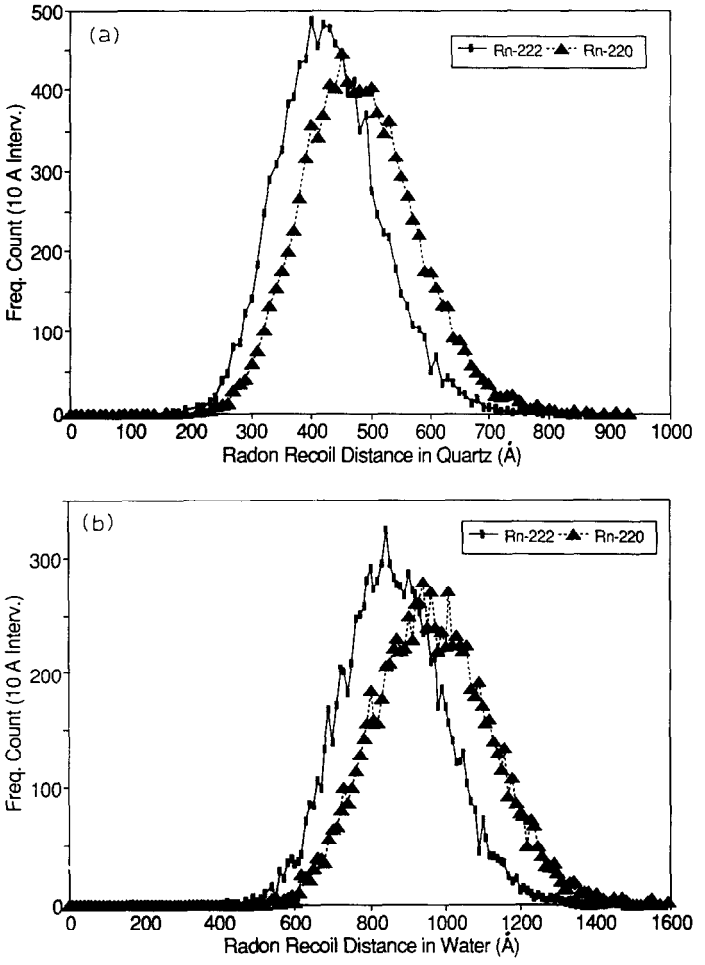


Fig. 1. Recoil range distribution curve of $^{222}$Rn and $^{220}$Rn. Total $10^4$ counts: (a) $^{222}$Rn and $^{220}$Rn within quartz; (b) $^{222}$Rn and $^{220}$Rn within water; and (c) $^{222}$Rn and $^{220}$Rn within air.

A porous medium can be described by a binomial indicator function:

$$U(x,y,z) = \begin{cases} 0, & \text{pore} \\ 1, & \text{solid} \end{cases} \tag{1}$$

The distribution of the pores (0's) and solids (1's) can be characterized by a probability density function (PDF) and an autocorrelation function (ACF) (Joshi, 1974). This distribution can be treated as a binomial random field. Therefore, by simulating a binomial field with the desired PDF and ACF properties, a synthetic porous medium is developed with the same characteristics as a real porous medium (Adler, 1992). The surface area of the pores can be counted over the synthetic porous medium with different measuring scales. The turning bands method (TBM) can be applied to simulate

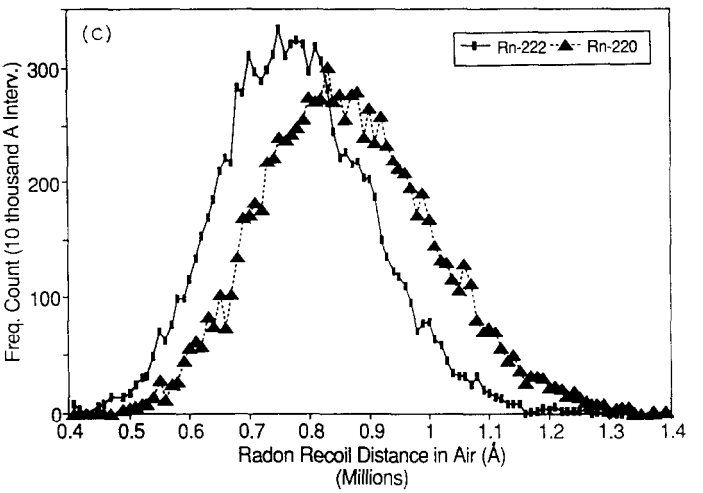


Fig. 1 (continued).

the synthetic porous medium. The TBM is a popular numerical technique which generates the replicate 3-D spatially correlated field by combining values found from a series of one-dimensional simulations along lines radiating outward from a coordinate origin (Tompson et al., 1989). The simulation is to calculate the field spectrum from the Fourier transformation of a covariance function. Then, the line spectrum is calculated from the field spectrum. Eventually, the realization of the desired random field is projected from all the line values simulated. This process will generate a random field with a Gaussian PDF and a specified ACF. If the desired random field does not have a Gaussian PDF, then a ACF transformation need to be conducted first from the method proposed by Joshi (1974) before applying the turning bands simulation. The Gaussian field is transformed into a binomial field (0,1) by setting a threshold value (which is the porosity value, e.g. 40% porosity, $z = -.255$ from the normal distribution table). The reason spatially correlated normal field can be transformed into a porous medium binary field is by the reasoning that the light intensity values scanning through a thin section. The pores, edges and matrix of a porous medium thin section have different light intensity values. These values can be assumed as having a Gaussian distribution or can be transformed into a normal distribution (Quiblier, 1984).

Table 1
Probability of single ion recoiling out of solid (quartz as host material) within certain distance from the surface

| Distance (Å) | 50 | 100 | 200 | 300 | 500 | 800 | 1,100 | 1,300 |
|---|---|---|---|---|---|---|---|---|
| Ion | | | | | | | | |
| $^{222}Rn$ | 0.4457 | 0.3928 | 0.3181 | 0.2700 | 0.1788 | 0.1113 | 0.0785 | 0.0681 |
| $^{220}Rn$ | 0.4340 | 0.4000 | 0.3329 | 0.2865 | 0.1996 | 0.1255 | 0.0875 | 0.0775 |

1 Å = $10^{-1}$ nm.

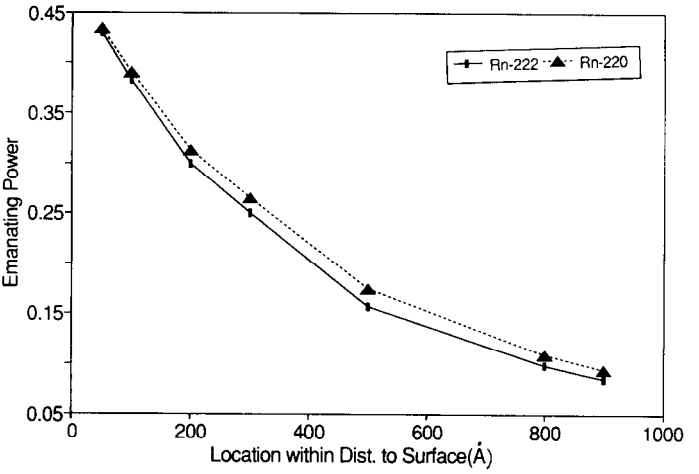


Fig. 2. Emanating power of $^{222}$Rn, $^{220}$Rn recoil out of quartz within certain distance from the surface.

In our example study, assume $\alpha$ is the variance, $\beta_i$ is the correlation scale, the random field we designed has a Gaussian PDF and the following exponential decay function:

$$\mathrm{Cov}(L) = \alpha^2 \exp\left[ -\left( \frac{l_1^2}{\beta_1^2} + \frac{l_2^2}{\beta_2^2} + \frac{l_3^2}{\beta_3^2} \right)^{1/2} \right] \tag{2}$$

TBM thus generates a 3-D spatially correlated normal field with the spatial covariance as a function of separation distance $L$. The porous medium can be transferred by setting up the proper threshold values.

Homogenous isotropic porous media (Fig. 3) are generated by using correlation structures $\beta_1 = \beta_2 = \beta_3 = 1$ and $\beta_1 = \beta_2 = \beta_3 = 3$ units and one unique spatial covariance function in the example. The grain size distributions can be manipulated by changing the correlation scales.

With the simulated synthetic porous media, the surface area of the pores can be counted. Because a porous medium has fractal properties, the surface area is scale dependent (Feder, 1988; Semkow, 1991). From the synthetic porous media, the surface areas of the grains are counted at different measuring square scales by using different area measuring boxes (with area units equals to 1, 4, 9 and 16 square units in the example) walking through the pores of the synthetic porous media. The log-log counted surface area values vs. the measuring scales can be projected to calculate the surface area at any designed scales. If $S_a(\delta)$ is assumed to be the surface area of a porous medium, $\delta$ (square unit) is area measuring scale, $a_0$ is the surface area when measuring scale is one unit, $D$ is the fractal dimension, based on the number–size relation between surface area of the porous media and the measuring scales $S \approx Nr^2$ (Feder, 1988), we have:

$$S_a = a_0 \delta^{(2-D)/2} \tag{3}$$

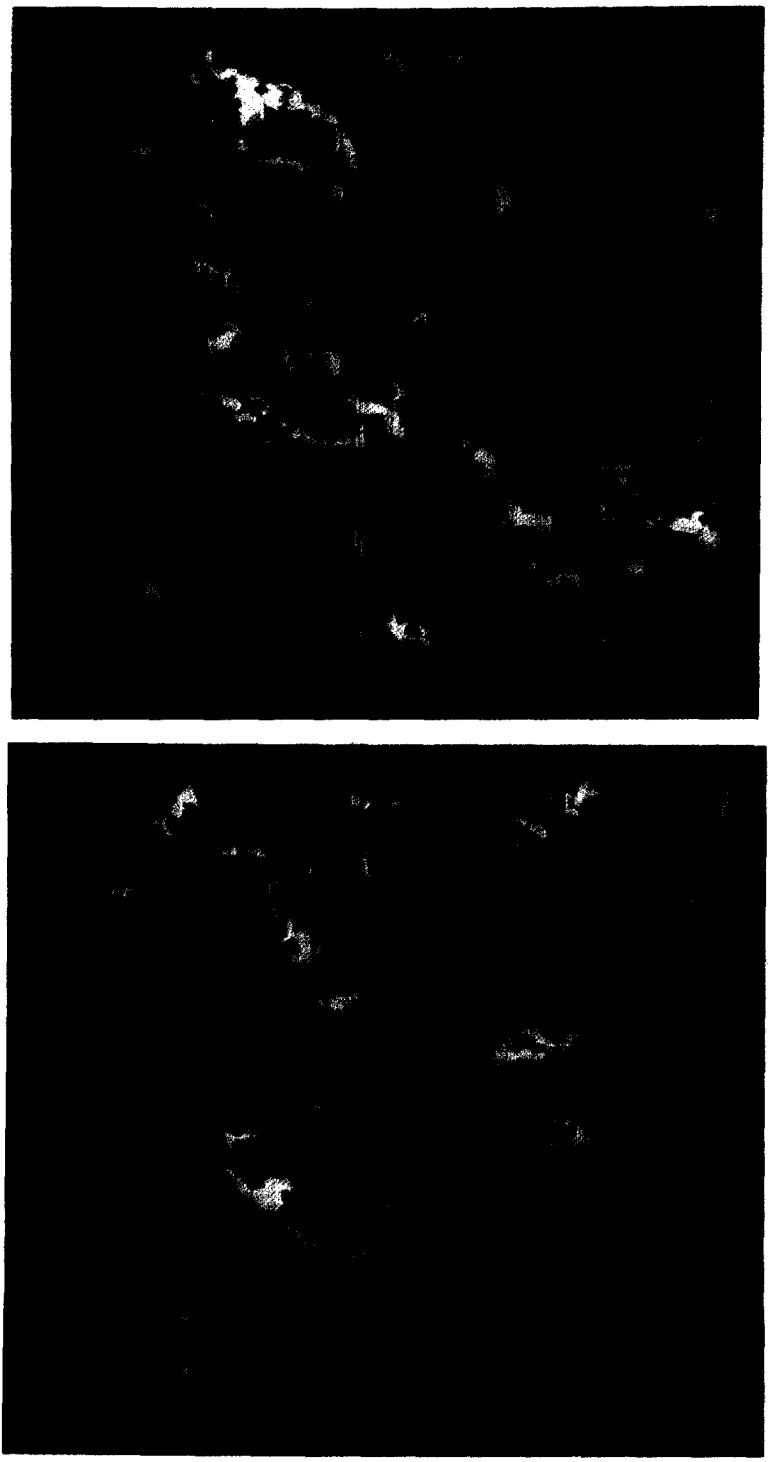

Fig. 3. Cross-sections of the simulated 3-D homogeneous, isotropic porous texture: (a) correlation scale $\beta = 1$; and (b) correlation scale $\beta = 3$. Simulated sample volume is $1 \times 1 \times 1$ mm$^3$, 50% porosity.

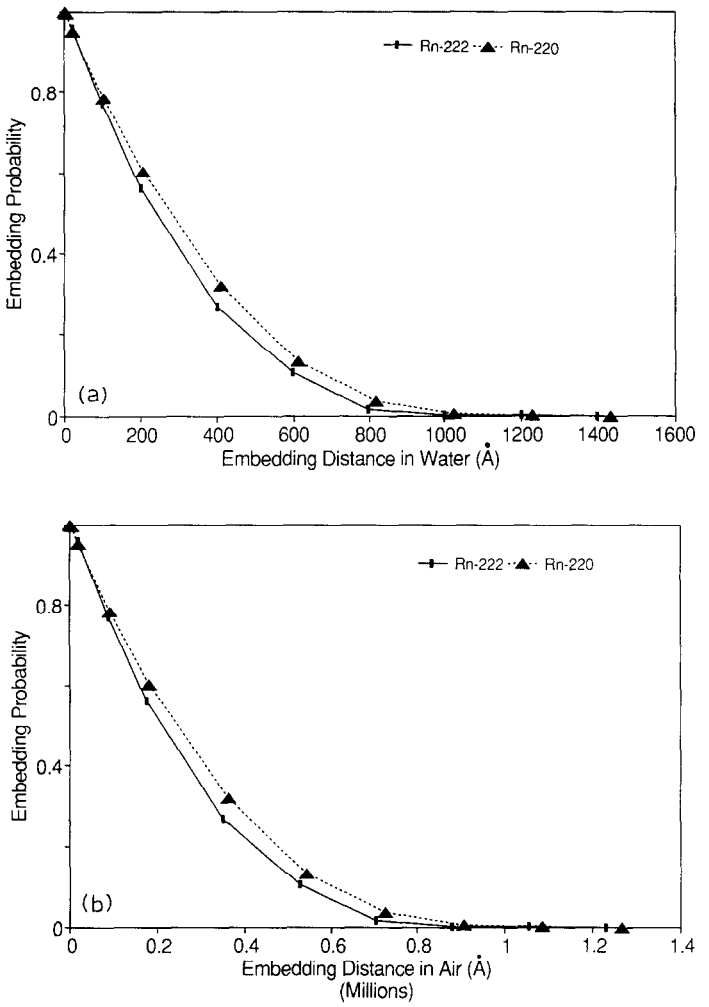


Fig. 4. The embedding probability $(1 - f_w)$ from Eq. 7 for recoiling radon vs. $x_w$, the distance it travels within water (or air) after it recoils out of solid: (a) in water; and (b) in air.

The fractal dimension of the isotropic and anisotropic synthetic homogeneous porous media with different porosities as defined by Eq. 3 has an average of 2.78. This result is within the range discussed by Semkow (1991).

## 4. Calculation of effective recoil surface areas

The recoil emanation rate not only depends on the surface area of the pores, but also depends on how close the pore surfaces are to one another. If the pore is very small, and the opposing surfaces are close, the recoiled daughter might embed into the adjacent

surface. Thus, only the recoiled radon staying in the water or air phase for free diffusion is considered as emanated. The recoiled radon passing through the water and air phase into a nearby solid is considered as embedded. When considering surface area of the pores as the initial recoil surface areas, the closeness of the nearby surfaces must be considered in order to subtract the embedding effect.

Assume $S_0$ is the surface area measured with scales above the maximum recoil length of radon within air or water without embedding effect. Assume $\Delta S_n$ is the surface area increase of $S_n$ over $S_{n-1}$ for decreasing measuring scale, $f_n$ is the fraction of $\Delta S$ contributing to emanation, and $S_w$ is the effective recoil surface area with water or air buffer $S_w$ after subtracted the embedding effect. Then we have:

$$S_w = S_0 f_0 + \Delta S_1 F_1 + \Delta S_2 f_2 + \Delta S_3 f_3 + \ldots + \Delta S_n f_n \tag{4}$$

If we assume that $P_{xn}$ is the probability of recoil ions which can reach $x_n$ distance within water after it recoils out of the solid, $f_i$ can be estimated according to the probability of the recoil energy left after the recoil ion recoils out of the solid phase. By using the recoil range distribution and the emanating power discussed earlier, we have:

$$f_w = 1 - P(x \geq = x_w) = 1 - (P_{xn} + P_{xn-1} + \ldots + P_w) \tag{5}$$

where $P_w$ can be obtained through the correlation to the probability of the ion recoil embedding distance $x_s$ within the same material (solid) by:

$$\frac{x_s}{x_w} \approx \frac{r_s}{r_w} \tag{6}$$

where $x_w$ is the distance the recoil ion traveling in water or air after the ion recoils out of the solid; $r_s$ is the average ion recoil distance in the solid; and $r_w$ is the average ion recoil distance in the water or air (Fig. 4).

## 5. Effective recoil surface area calculation given the moisture content

Under either saturated or dry conditions, a single layer of buffer exists with either water or air filling the pore space completely. Eq. 4 can be implemented by following through the above discussion. In a partially saturated condition, both the air and water buffers coexist. Water is retained in certain part of the pores, and the air in another part. The calculation of the effective recoil surface area therefore needs to consider both the quantity and distribution of moisture in the pores.

In a condition of partial saturation, the water is retained in the pores by capillary forces. The stronger the capillary force, the more water can be retained in the pores. If we assume that the atmospheric pressure equals zero, the pore radius is $r$, and the surface tension of water is $\sigma$, the capillary force, $P_c$ is given by Laplace equation $P_c = -2\sigma/r$. Therefore, the capillary force is inversely proportional to the radius of the pores. The last pores from which the water drains are the smallest pores. Therefore, the water occupies the smaller pores, and the air occupies the bigger pores.

The recoil surface area Eq. 3 is deduced from fractal calculation. Each $\Delta S$ increase is the result of a decreasing scale of $\Delta\delta$. The increased surface areas are the sum of the

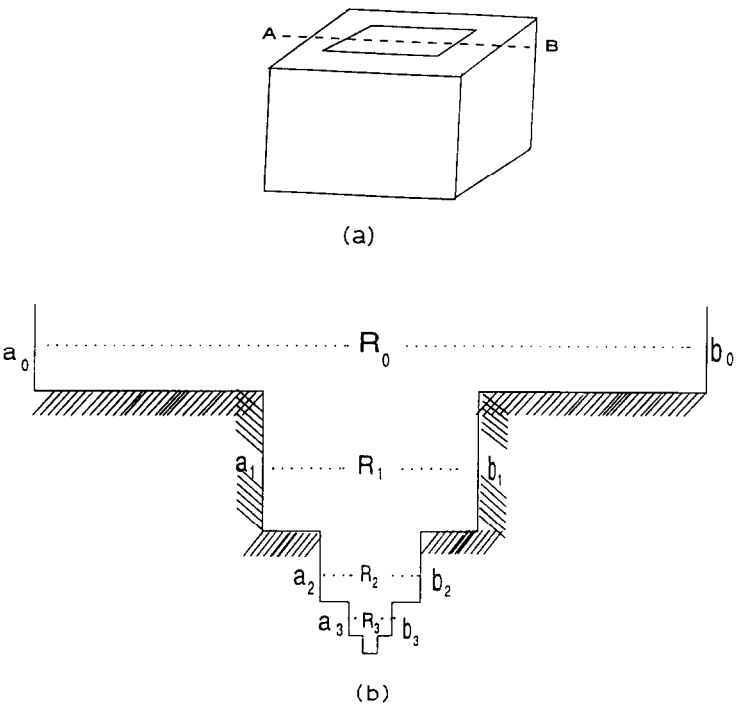


Fig. 5. Idealized cross-section picture schematically showing the surface area counting scheme. Scale decreases from $R_1$ to $R_2$ (for area, should be square), the area increase in one direction ($A-B$ cross-section direction) is $a_2$ and $b_2$. a. Cubic cell with an idealized pore. b. Cross-section of the idealized pore from $A$ to $B$.

surface areas of four sides of new small sized boxes reached by smaller scales. The reason only four sides are counted as newly increased is because the top and bottom are not newly increased areas in our counting practice (Fig. 5). Assume $P^{v,b_i}$ is the volume percentage taken by side length $b_i$ (equals $\delta_i^{1/2}$) cube, and $\Delta S_i$ is the surface area increase for a scale change from $\delta_{i+1}$ to $\delta_i$ by $\Delta\delta$, $V$ is the total sample volume and $\eta$ is the porosity of the sample, then in a statistic sense, we will have:

$$P^{v,b_i} = \frac{\Delta S_i b_i}{4V\eta} \tag{7}$$

Assume the smallest initial scale is $b_0$ (which is $\delta_0^{1/2}$), up to measuring scale $b_k$, from Eq. 7 the total volume taken by size $b_0$ to $b_k$ cubes will be:

$$P_{1,k}^{v,b_i} = P^{v,b_0} + P^{v,b_1} + \ldots + P^{v,b_k} = \frac{(\Delta S_0 B_0 + \Delta S_1 b_1 + \ldots + \Delta S_k b_k)}{4v\eta}$$

$$= \frac{\sum_{i=0}^{K} \Delta S_i b_i}{4v\eta} \tag{8}$$

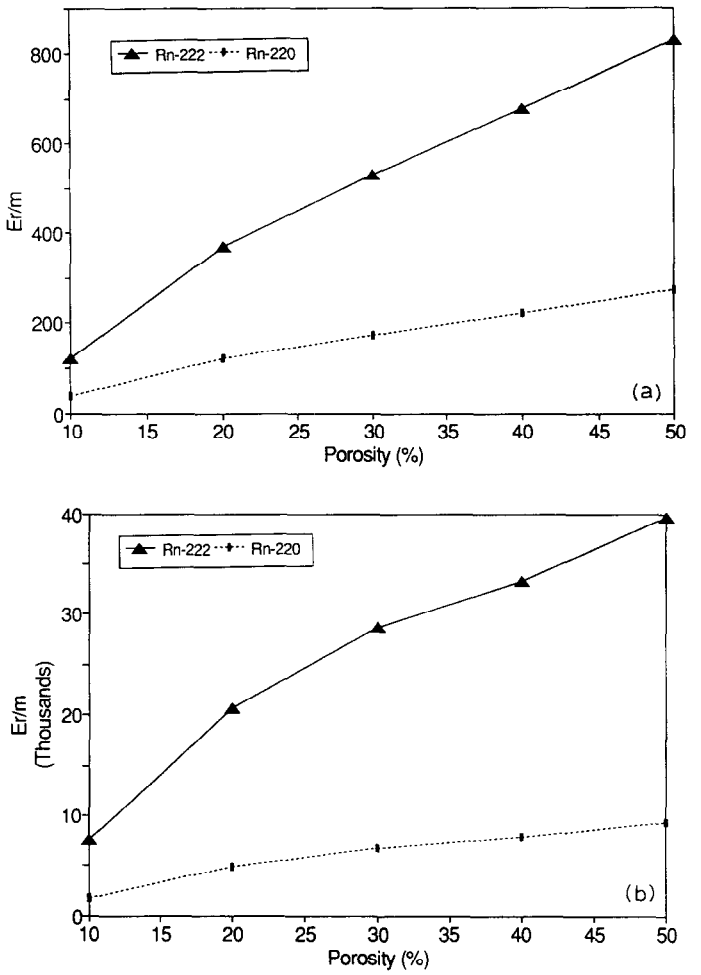


Fig. 6. The expected radon emission rate vs. porosity plot for 1 kg of quartz host sample with 0.1% of $^{238}U$ and $^{232}Th$: (a) dry sample; (b) ~10% moisture; (c) ~18% moisture; and (d) saturated sample.

The moisture content ($\theta$) is defined as the percentage of the pores occupied by water. Because the moisture occupation within the pores starts from the fine pores to big pores, the volume percentage $P_{1,k}^{v,b}$ can be considered as the moisture occupation percentage of all these sizes $b_0$ to $b_k$ pores. $\theta = P_{1,k}^{v,b}$. Conversely, given the moisture content $\theta$, the volume percentage can be determined. The measuring scales for the pore size up to this volume percentage can be defined. Then $\Delta S_i$ can be determined from Eq. 8 given the moisture content.

In a partially saturated condition, the pores are divided into those parts, occupied by water and those occupied by air. As discussed earlier, normally the water occupies the fine pores and air occupies the relatively large pores. Thus when the measuring scale is below a certain size, the pores will be occupied by water and above a certain size by air.

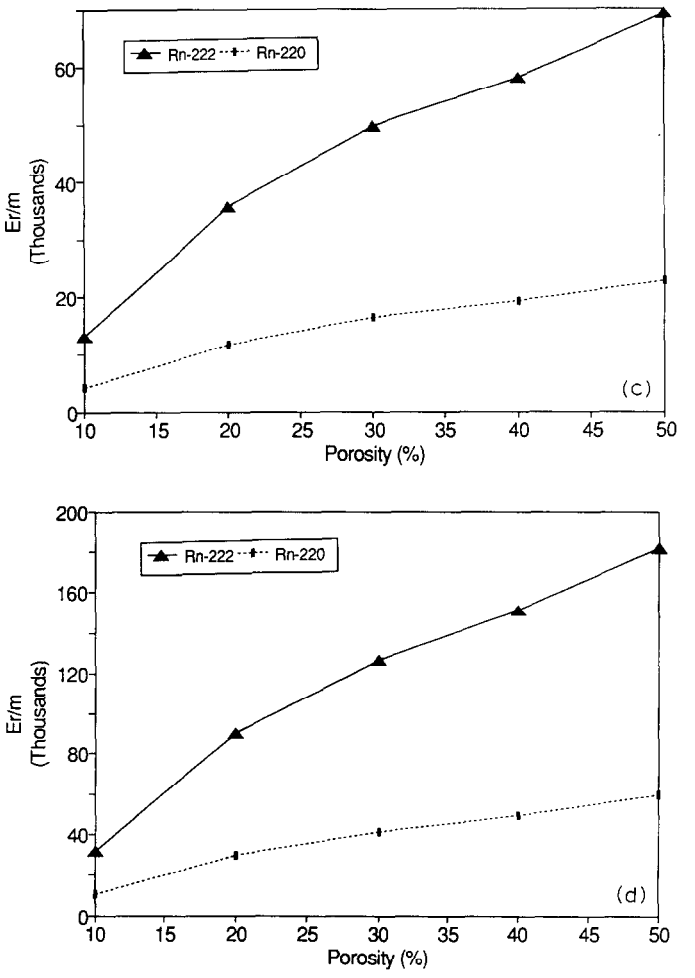


Fig. 6 (continued).

Above a certain measuring scale, the $\Delta S$ will correspond to the air embedding probability and below a certain scale, the $\Delta S$ will correspond to the water embedding probability. Therefore, the effective recoil surface areas for Eq. 4 can be calculated given the moisture content.

## 6. Radon emanation rate versus moisture content change in porous media

After the effective recoil surface area is calculated, the total ion numbers located within the effective recoil range can be calculated. Assume $E_r$ is the emanation rate of a recoil daughter (atoms $min^{-1}$), $P_s$ is the recoil probability of a single daughter within

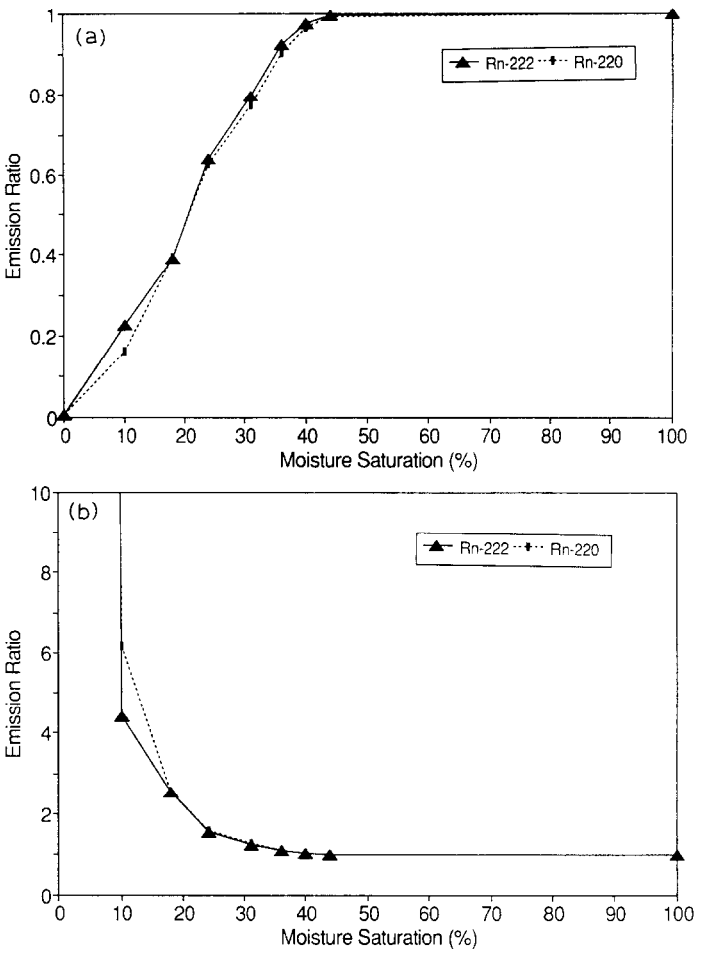


Fig. 7. Radon emission ratio at different moisture content to saturated condition, vs. approximate moisture content plot at 30% porosity: (a) ratio of $E_{moi.}/E_{sat.}$ (refer to emission ratio of different moisture to saturated): and (b) $E_{sat.}/E_{dry}$.

the effective recoil range, $A_p$ is the activity of the parent radioactive element, the emanation rate is:

$$E_r = A_p P_s \tag{9}$$

where if assume radioactive equilibrium, $A_p$ will be equal to:

$$A_p = \frac{f\rho(\mathrm{mr})S_a}{M_p} c\lambda \tag{10}$$

where $f$ is the weight percentage of $^{238}U$ or $^{232}Th$ in the host material; $\rho$ is the density of the material (g cm$^{-3}$); $S_w$ is the effective recoil surface area of the sample (cm$^2$); mr is the average effective recoil thickness (less than the maximum recoil range $8 \cdot 10^{-6}$

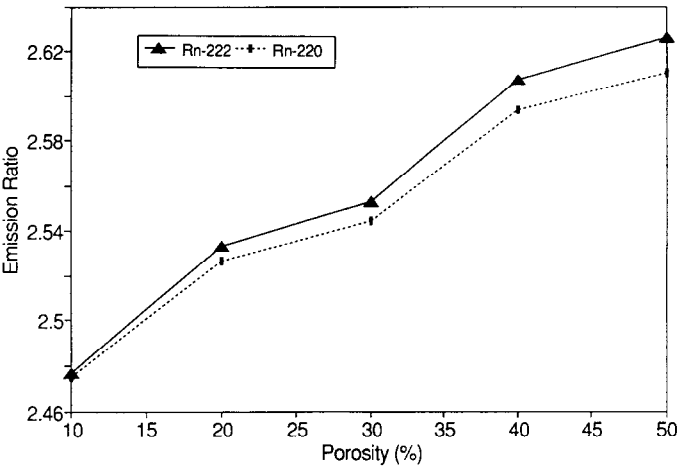


Fig. 8. Radon emission ratio at 18% moisture content to saturated condition vs. porosity plot.

cm); $\lambda$ is the decay constant ($min^{-1}$) of $^{238}U$ or $^{232}Th$; $M_p$ is the atomic weight of the $^{238}U$ or $^{232}Th$; $c$ is $6.022 \cdot 10^{23}$ which is the Avogadro number. Most of the parameters listed above can be practically determined except the effective recoil surface area, which can be statistically calculated from Eq. 4.

By substituting Eq. 4 into Eqs. 9 and 10, the radon emanation rate under different moisture contents can be calculated (Fig. 6). The ratios of the emanation rate under different moisture contents to the emanation rate under a saturated condition vs. moisture content change can be calculated (Fig. 7). The emanation ratio shows a increasing trend with increased porosity for the same material weight and the same moisture content (Fig. 8). This relationship develops because as the porosity increases the effective recoil surface area increases also. From the calculation, the recoil emanation rate of radon under a saturated condition is much larger than the recoil emanation in a dry condition. This result stems from the fact that the recoil range of radon within air is $\sim 880$ times larger than in water. Water is much more effective in trapping recoil radon than air. With a small quantities of water in the pores, the emanation rate dramatically increases. As the moisture content increases to a range of 30–40%, the emanation rate is almost the same as the emanation rate in a saturated condition (Fig. 7). This result is expected at moisture content above 30%, because a thin film of water will cover most of the pore surface due to the capillary forces. This thin film of water will be thick enough to stop the recoil daughters within the water (remember for the $\alpha$-particle experiment, a sheet of paper is enough to stop all the radiated $\alpha$-particles which have a much higher energy than the recoil daughters).

Keep in mind that the adsorption of water on the rough surface in real media is much more complicated than the case we modeled. As some researchers have already pointed out, there might be a layer of water on all surfaces of the pores even under a very low moisture content (Waldron et al., 1961). This condition might imply that our calculation while correct for saturated and dry conditions, might slightly underestimate the moisture

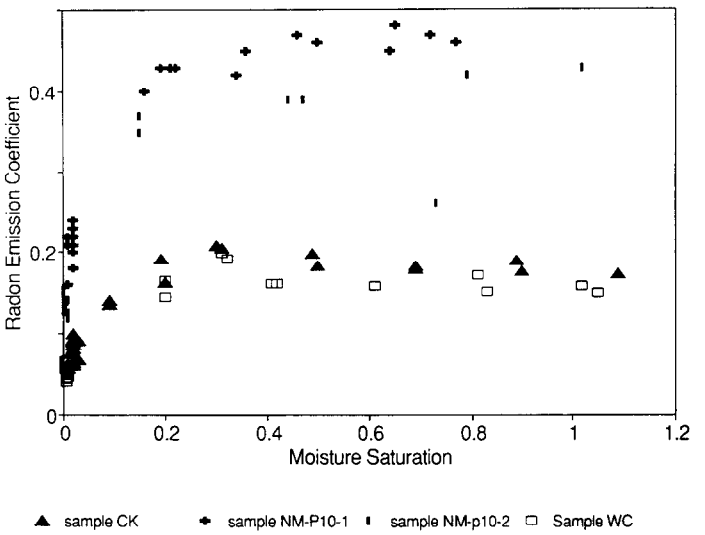


Fig. 9. Measured emission coefficients vs. moisture saturation plot. Data are extracted from four samples in Thamer et al.'s (1982) report.

coverage in the pores for the conditions of partial saturation. It seems that a slight adjustment of the curve of Fig. 7 to the left would be appropriate. Also the water film thickness depends on the temperature and humidity (L.H. Lee, pers. commun., 1994), these can make the calculation of radon recoil at a unsaturated condition even more complicated than it already is.

## 7. Comparison with existing experimental data

Thamer et al. (1982) conducted an experiment to measure the emanation coefficients under dry and wet conditions. For the wet experiment, a sample with a designed moisture content was sealed in a can for $\sim 30$–$60$ days. Having reached equilibrium, the sample was counted for $(R_1)$ in a Gamma scintillation detector. The sample was dried in a vacuum, and subsequently counted for $(R_2)$. The wet emanation coefficient is:

$$E_m = (R_1 - R_2)/R_1$$

The dry experiment was conducted in the same manner to provide $(R_3)$. After the sample was de-emanating by vacuuming, it was counted for $(R_4)$. The dry emanation coefficient is:

$$E_d = (R_3 - R_4)/R_3$$

These ratios are the radioactivities of radon suspended in the moisture or air for free diffusion after the radioactive elements reach equilibrium to the radioactivity of radon originated from the sample itself. The higher the ratio, the more retained radon in the moisture.

Four representative data sets are extracted from their experiments (Fig. 9). The general trend of the emanation ratios of Figs. 7 and 9 matches well. As the moisture content increases above 5%, the recoil emanation approaches the rate of saturation asymptotically. Upon reaching 30% of the moisture, it is close to reaching the recoil rate of saturated conditions. This result shows that the radon emanation rates are positively correlated with the moisture saturation rate as our simulation proved.

## 8. Summary

This paper presents a theoretical calculation of the recoil emanation rate under different moisture content conditions. Based on the nuclei collision theory, the modified TRIM program is used to calculate the detailed recoil range distribution of radon in solid, water and air three phases. The recoil surface area of porous media is calculated through the fractal measurement over a simulated synthetic porous media generated by turning bands method. The embedding effect is solved by calculating the non-embedding probability and the effective recoil surface area. By using the relation of the measuring scale and the capillary force principles, the moisture content counting is solved. The theoretical calculation proves that the moisture saturation has a clear effect on the radon emanation rate. The moisture saturation is positively correlated with the radon emanation rate. Water has a much powerful trapping recoil radon efficiency than air. As the moisture content increases, the emanation rate increases steadily and at $\sim 30$–$40\%$ moisture content the emanation rate is about the same rate as under the saturated conditions. At $\sim 30\%$ saturation, a water film will completely cover the mineral surfaces. This film is thick enough to trap the recoiled ions in water. The theoretical emanation ratio also shows a good compliance with the experimental emanation coefficient trend from Thamer et al. (1982).

## Acknowledgements

The authors are grateful to Geology Department, the Florida State University for its support of the this project. The authors wish to thank J. Cowart, K. Osmond, M. Koch, S. Kish and R. Odom all from Florida State University for their support of this project.

## References

Bossus, D.A.W., 1984. Emanating power and specific surface area. Radiat. Prot. Dosimetry, 7: 73–76.

Brookins, D.G., 1990. The Indoor Radon Problem. Columbia University Press, New York, NY, 229 pp.

Drever, J.I., 1988. The Geochemistry of Natural Waters. Prentice Hall, Englewood Cliffs, NJ, 437 pp.

Feder, J., 1988. Fractals. Plenum, New York, NY, 283 pp.

Joshi, M.Y., 1974. A class of stochastic models for porous media. Ph.D. Dissertation, University of Kansas, Lawrence, KS, 150 pp.

Paulsen, R.T., 1991. Radionuclides in groundwater, rock and soil, and indoor air of the northeastern united states and southeastern Canada — A literature review and summary of data. In: Field Studies of Radon in Rocks, Soil, and Water. U.S. Geol. Surv., Bull. No. 1971, pp. 195–225.

Quiblier, J.A., 1984. A new three-dimensional modelling technique for studying porous media. J. Colloid Interface Sci., 98: 84–102.

Semkow, T.M., 1990. Recoil–emanation theory applied to radon release from mineral grains. Geochim. Cosmochim. Acta, 54: 425–440.

Semkow, Y.M., 1991. Fratal model of radon emanation from solids. Phys. Rev. Lett., 66: 3012–2015.

Tanner, A.B., 1980. Radon migration in the ground: A supplementary review. In: T.F. Gesell and W.M. Lowder (Editor), The Natural Radiation Environment III, Symposium Proceedings, Houston, Texas, April 1978, Vol. 1. U.S. Dep. Environ., Natl. Tech. Info. Serv., Washington, DC, Rep. CONF-780422.

Thamer, B.J., Nielson, K.K. and Felthauser, K., 1982. The effects of moisture on radon emanation including the effects on diffusion. U.S. Dep. Inter., Rep. Bur. Mines OFR 184-82, Natl. Tech. Info. Serv., Washington, DC, Rep. PB83-136358.

Tompson, A.F.B., Ababou and Gelhar, L.W., 1989. Implementation of the three-dimensional turning bands random field generator. Water Resour. Res., 25: 2227–2243.

Waldron, L.J., McMurdie, J.L. and Vomocil, J.A., 1961. Water retention by capillary forces in an ideal soil. Soil Sci. Soc. Am. Proc., 25: 265–267.

Ziegler, J.F., Biersack, J.P. and Littmark, U., 1985. The Stopping and Range of Ions in Solids. Pergamon, Oxford, 321 pp.